Article

Atomic Stripe Formation in Infinite-Layer Cuprates

Yoshiharu Krockenberger,* Ai Ikeda, and Hideki Yamamoto

ACCESS | Metrics & More | Article Recommendations | SI Supporting Information

ABSTRACT: High-temperature superconductivity appears in cuprate materials that have been tuned in a way where the copper−oxygen bond configuration and coordination is in a state of minimal energy. In competition with the Jahn−Teller effect, which impedes the formation of infinitely connected CuO_2 planes, the state of minimal energy persists for planar copper−oxygen bond length variations of up to 10%. We have synthesized the infinite-layer phases of $CaCuO_2$ and $SrCuO_2$ as single-crystalline films using molecular beam epitaxy and performed in-plane scanning transmission electron microscopy mapping. For the infinite-layer phase of $CaCuO_2$ with a short Cu−O bond length, the CuO_2 planes maintain their minimal energy by forming distinguished atomic stripes. In contrast, atomic stripe formation does not occur in the infinite-layer phase of $SrCuO_2$, which has a larger Cu−O bond length. The polar field provided by the charge reservoir layer in cuprates with infinitely connected CuO_2 planes holds the key over the emergence of superconductivity and is vital to maintain infinitely connected CuO_2 planes themselves.
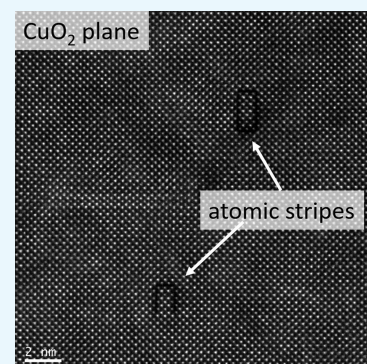
INTRODUCTION

Cuprate superconductors have not lost their charm even after decades of research. This attention is borne out of the uniqueness that a certain set of spin, charge, and orbital degrees of freedom allow for superconducting transition temperatures under ambient pressure well in excess of the boiling temperature of liquid nitrogen. In transition-metal oxide (TMO) interfaces, the diverging lattice, electronic, orbital, and magnetic behaviors of the two adjacent materials lead to properties that are commonly diverse from those of the two individual bulk materials and this is not different for high-temperature superconducting cuprates. This would imply that one were at the brink to tailor and pitch the net electronic response behavior of interfaces. Much effort has been focused on the investigation of single individual interfaces while cuprate superconductors are built up from at least two or more interfaces. Cuprate superconductors are natural superlattices, composed of copper-oxide planes and planes of oxides, so-called charge reservoir layers (CRLs), with the sole function to shift the instability of tenorite[1,2] toward CuO_2 planes. In other words, the CRLs have the power to transform the monoclinic angle $\beta = 99.467°$ of the tenorite crystallographic unit cell toward 90° in cuprate superconductors. The fact that the crystal structure and consequently its electronic response does not follow the trend set by other simple $3d$ TMOs is the consequence of a not yet well-understood interplay of electronic, spin, lattice, and orbital degrees of freedom.

In cuprate superconductors, the CRLs are made of rare-earth, alkaline earth, or post-transition-metal oxide strata that sandwich the CuO_2 planes. Nonetheless, this building principle finds its exception in cuprates with the so-called infinite-layer (IL) structure and simple cations, e.g., Ca^{2+} or Sr^{2+} ions,

separate adjacent CuO_2 planes. Within a unit cell, the charge-neutrality criteria must be fulfilled and this is the task of the CRL. Furthermore, charge-carrier doping into the CuO_2 planes from the CRL by heterovalent cation substitution is considered as the fall-back explanation for the induction of super-conductivity in cuprates. Regrettably, this seems not to function as expected for IL cuprates. In $IL-SrCuO_2$, trivalent rare-earth substitution (R^{3+}) induces superconductivity[3,4] though the opposite is true for $IL-CaCuO_2$[1,5] (Figure S1). The fact that $Sr_{1-x}R_x^{3+}CuO_2$ becomes superconducting and $Ca_{1-x}R_x^{3+}CuO_2$ does not is puzzling particularly under the light that both materials are of equally high crystalline quality (Figures S2 and S6) when prepared by molecular beam epitaxy (see the Supporting Information). Apparently, a yet to be quantified mechanism is responsible for this difference and motivated us to link the superconducting transition temperature T_c of all cuprate superconductors to their in-plane copper−oxygen bond lengths d_{Cu-O} (Figure 1) in a phase diagram. In this context, two singularities emerge for $d_{Cu-O} \approx$ 1.895 and 1.950 Å, where superconductivity is effectively suppressed no matter the circumstances. In detail, if $d_{Cu-O} \approx$ 1.950 Å, at the boundaries between zones I and II (Figure 1), it is not just the vanishing superconducting state; upon shortening d_{Cu-O}, the coordination of copper changes from square planar into a state where the copper coordination is
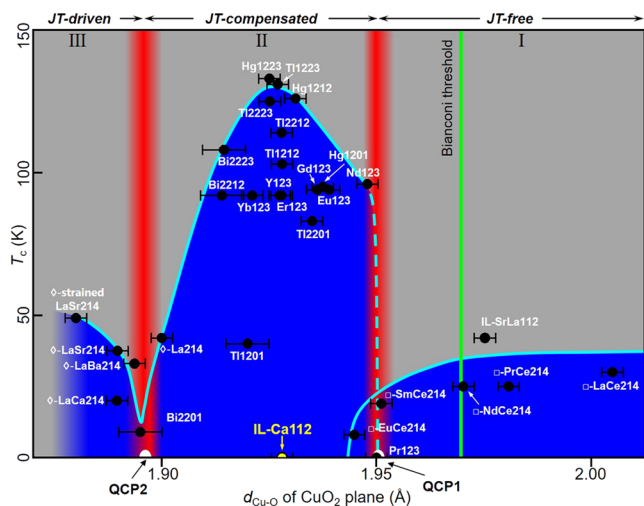
Figure 1. Phase diagram of cuprate superconductors where the superconducting transition temperature T_c is plotted as a function of d_{Cu-O} length for several cuprates. All compounds plotted here have infinitely connected CuO_2 planes and the listed cuprates do show superconductivity, except IL-CaCuO$_2$. In zones I and III, the coordination number of copper is unique, whereas all three coordinations may coexist in zone II. The Bianconi threshold is the length in the unstrained and undistorted CuO_2 plane.[14] For every Cu−O bond length between 1.850 and 2.000 Å, there exist a chemistry (typically called charge reservoir layer[15]) that induces superconductivity, and this superconductivity appears throughout the phase diagram except for two distinct points at 1.950 and 1.895 Å, quantum critical points (QCPs) I and II, respectively. Copper−oxygen bond length values have been taken from refs 16−19 and for $CaCuO_2$, $Sr_{1-x}La_xCuO_2$, R_2CuO_4, $La_{2-x}Sr_xCuO_4$, and $Bi_2Sr_2CaCu_2O_{8+\delta}$ are from our experiments. Cuprate superconductors containing copper in a square-planar coordination environment have vacant apical sites and such cuprates are therefore not susceptible to Jahn−Teller distortions (JT free in zone I). In contrast, the Jahn−Teller effect governs the entire formation of the crystal structure if copper is sixfold-coordinated (JT driven in zone III). Subtle deviations from an exact square-planar copper coordination cause a Jahn−Teller response that depends on the polarization field of the CRL above or below the CuO_2 planes, and cuprates in zone II are called "Jahn−Teller-compensated".

octahedral (O), pyramidal (P), or pyramidal (P) and square planar (S). At $d_{Cu-O} \approx 1.950$ Å, the criteria of a quantum critical point[6] are sufficiently fulfilled and we label it as the first quantum critical point (QCP 1) in the cuprate phase diagram. In terms of real cuprate materials, $PrBa_2Cu_3O_{7-\delta}$[a9] (P) and $Gd_{2-x}Ce_xCuO_4$[10] (S) represent QCP 1 under equilibrium conditions. Indeed, these two materials are not superconducting. Yet, this does not come as a surprise and is known for long. With further decreasing d_{Cu-O}, superconductivity disappears yet again, this time for $d_{Cu-O} \approx 1.895$ Å, which is between zones II and III in the phase diagram (Figure 1). For $d_{Cu-O} \approx 1.895$ Å, another transition in the coordination of copper takes place. This time it is from O or P, or P and S (zone II)[11] to exclusively O (zone III).[12] Again, also this point suffices the requirements set forth to qualify as a QCP, labeled QCP 2 in the cuprate phase diagram (Figure 1). The phase diagram shown here has been assembled from unstrained cuprate bulk materials. For thin materials, where epitaxial strain controls the polarization field of the CRL, the absolute position of QCP 1 and 2 may be freely manipulated and was shown for La_2CuO_4 thin films.[13] We note

that cuprate superconductors located in zone II have the highest T_c values, and discussions about the absolute magnitude of the superconducting transition temperature are beyond the scope of this manuscript. It is, however, quite more important to note that IL-CaCuO$_2$ has a d_{Cu-O} that puts it right in the center of zone II, while being neither a metal nor a superconductor (Figure S1). We conjecture two conclusions that can be drawn from the cuprate phase diagram. First, the chemistry of strata above and/or below the CuO_2 planes influences the equilibrium bond length of the Cu−O bond. In other words, as CRLs are made up of various ions having different effective polarization strengths, the Cu−O bond lengths are subjected to the competition between the intrinsic Jahn−Teller effect in Cu^{2+} that impedes the formation of infinitely connected CuO_2 planes and the extrinsically applied polarization strength. Second, there are critical copper−oxygen bond lengths where the superconducting transition temperature has vanished ($T_c = 0$ K). Independently, in the absence of such CRL or polarizing strata, the copper−oxygen bonding scheme succumbs entirely to what is dictated by the Jahn−Teller effect as seen in tenorite—the symmetry is lowered from tetragonal to monoclinic. To approach a solution as to why IL-CaCuO$_2$ is not superconducting, one needs to consider the model of an undistorted $(CuO_2)^{2-}$ plane without having to deal with influences stemming from polarization or strain, namely, bulk-like samples without CRLs. Using energy minimizing principles, Bianconi et al.[14] reported $d_{Cu-O} \approx$ 1.965 Å, for a free-standing CuO_2 plane, where Cu is square-planar coordinated and we define this length as "Bianconi threshold", d_B. Certainly, experimental verification of this value is a tough task although some groups report on tetragonal CuO ultrathin films[20−22] with d_{Cu-O} slightly (≈ 2 pm) shorter than the Bianconi threshold. More importantly is, however, the fact that cuprates with Cu−O bond lengths shorter than the Bianconi threshold[14] are susceptible to stripe order, quite in contrast to cuprates with longer Cu−O bond lengths.[23−27] Therefore, does IL-CaCuO$_2$ opt for stripes, too? Answering this question requires atomically resolved imagery of an ultrahigh-quality crystal.

■ RESULTS AND DISCUSSION

To achieve such IL-CaCuO$_2$ crystals, we used molecular beam epitaxy.[1] For comparability, we synthesized IL cuprates $CaCuO_2$, $SrCuO_2$, and their siblings, where Ca has been substituted by 4% of Nd and Sr by 10% of La, respectively. Cross-sectional scanning transmission electron spectroscopy (STEM) images (Figure S6) of IL-Ca$_{1-x}$R$_x$CuO$_2$ and IL-Sr$_{1-x}$R$_x$CuO$_2$ confirm that these materials are, indeed, free of impurity phases or stacking faults. While those images are on the cation arrangements and, in principle, insensitive to possible defects related to oxygen sublattice imperfection, our specimens are reasonably free from such defects. It is widely known that some different phases are readily formed and contaminated the IL cuprate phase. Such impurity phases are also subject to the applied annealing conditions. Consequently, we applied the criteria of phase purity, which is a sufficient measure for oxygen sublattice perfection.[5] Unfortunately, information from cross-sectional STEM alone is insufficient as it presents only a marginal snapshot of the copper−oxygen plane. Instead of cross-sectional STEM images, in-plane STEM images (see the Supporting Information) may unearth hidden distortions that are the result of the competition between the Jahn−Teller effect and the polar-
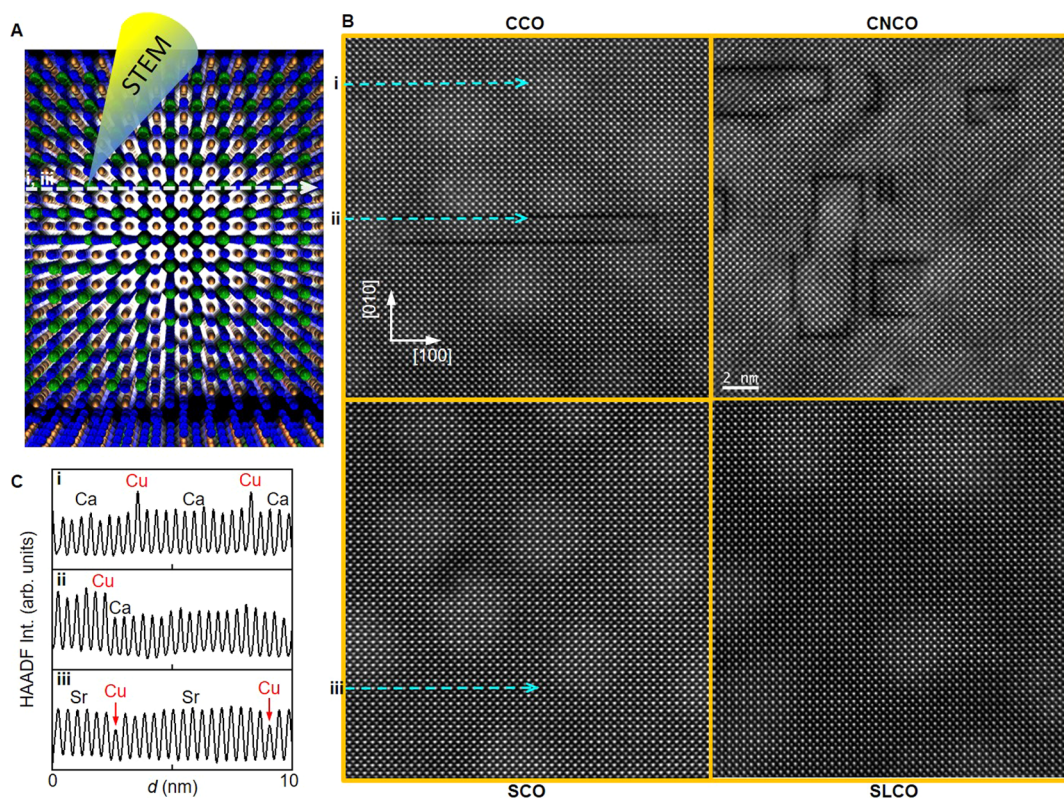
Figure 2. Cationic stripe formation in the CuO_2 planes of the infinite-layer $CaCuO_2$ system revealed by in-plane STEM mapping. (A) Perspective view on the CuO_2 plane of the infinite-layer cuprate with the tetragonal crystal structure ($P4/mmm$, S.G.: 123) of $CaCuO_2$. The dashed line is the scanning position and direction shown in (B) and the STEM intensity profiles are plotted in (C). The STEM scanning path in between two adjacent Cu sites and the detected element would be only Ca. (B) High-resolution cross-sectional transmission electron microscopy images taken of $CaCuO_2$ and $Ca_{0.96}Nd_{0.04}CuO_2$ grown on (001) LSAT substrates, $SrCuO_2$ on (001) $SrTiO_3$, and $Sr_{0.90}La_{0.10}CuO_2$ thin film grown on (110) $DyScO_3$ substrates. In (C), STEM intensity line scans taken at locations (i), (ii), and (iii) positions shown in (B) are plotted as a function of distance. Cationic stripes are formed in $CaCuO_2$ but not in $SrCuO_2$. In superconducting cuprates with a well Jahn–Teller-compensated CRL, e.g., $Bi_2Sr_2CaCu_2O_{8+\delta}$, stripes within the CuO_2 planes are also not observed (Figures S2 and S3). Cross-sectional scanning transmission microscopy images of IL-$CaCuO_2$ and IL-$SrCuO_2$ are shown in Figure S6.

ization fields which extend their influence on the CuO_2 planes. Accordingly, and we have taken high-resolution in-plane images (Figure 2) of the bare CuO_2 planes. These images reveal principally the CuO_2 plane, though there is more. For IL-$CaCuO_2$ and IL-$Ca_{0.96}Nd_{0.04}CuO_2$, the CuO_2 plane is blotched with rabbets, i.e., antisite boundaries, linear in shape with 90° corners. It is plausible that these CuO_2 planes ease their internal stress by forming rabbet structures and therefore the rabbet structures do form in IL-$Ca_{1-x}R_xCuO_2$ while they are absent in IL-$Sr_{1-x}R_xCuO_2$. In other words, cationic stripes formed for $d_{Cu-O} < d_B$ but not for $d_{Cu-O} > d_B$. Independently, atomically resolved, element-specific line scans using energy-dispersive spectroscopy (Figure 2) verify that the Ca–Cu order has been upended (Figure 2, line scan (ii)) while forming rabbets and these rabbets have therefore a cationic character. In contrast, the oxygen position remains intact (Figure 3D). While anionic stripe formation is not seen for the IL-$Ca_{1-x}R_xCuO_2$ system, it is throughout possible and has been reported for doped oxygen anions in $HgBa_2CuO_{4+\delta}$.[28] More importantly here is, however, that these cationic stripes are strong enough to sustain even with doping of 4%, as exemplified by atomically resolved, element-specific STEM images of IL-$Ca_{0.96}Nd_{0.04}CuO_2$ in Figure 3. The mechanism of cationic stripe formation is schematically visualized in Figure 3G, where a half-unit cell shift of the CuO_2 planes along the boundary gives rise to cationic stripes linked to structural

dimorphism in the form of partially disordered nanoscale stripes.[14,29]

After all, why do these cationic stripes form in IL-$Ca_{1-x}R_xCuO_2$ and are not seen in cuprates with comparable d_{Cu-O}, e.g., $Bi_2Sr_2CaCu_2O_{8+\delta}$ (Figures S2 and S3)? To answer this question, the polar character of the cuprates, where doubly negatively charged CuO_2 planes $(CuO_2)^{2-}$ are sandwiched by doubly positively charged CRL $(A_xO_y)^{2+}$ (A are chemical elements), has to be considered. Furthermore, real crystalline materials are inevitably subject to crystallographic imperfections[30−33] and the resultant charge imbalance must be compensated within the smallest possible volume.[34] However, these considerations must incorporate also the impact of the Jahn–Teller principle in these cuprates[35] as local geometric arrangements of the O^{2-} ligands dictate them. Due to octahedral coordinated copper, cuprates in zone III (Figure 1) are subject to Jahn–Teller distortions and are built up from infinitely connected CuO_6 strata with massively elongated c-axis lengths; in zone III, the Jahn–Teller distortions are therefore explicit. Nonetheless, despite strong Jahn–Teller interventions in zone III, additional distortions—tilted CuO_6 octahedrons—are well known, for example, for $La_{2-x}Sr_xCuO_4$ and $La_{2-x}Ba_xCuO_4$.[36] Accordingly, cuprates in zone III have sufficient means to compensate for crystal imperfections without harming the CuO_2 planes. A prominent example where these mechanisms result in total loss of super-
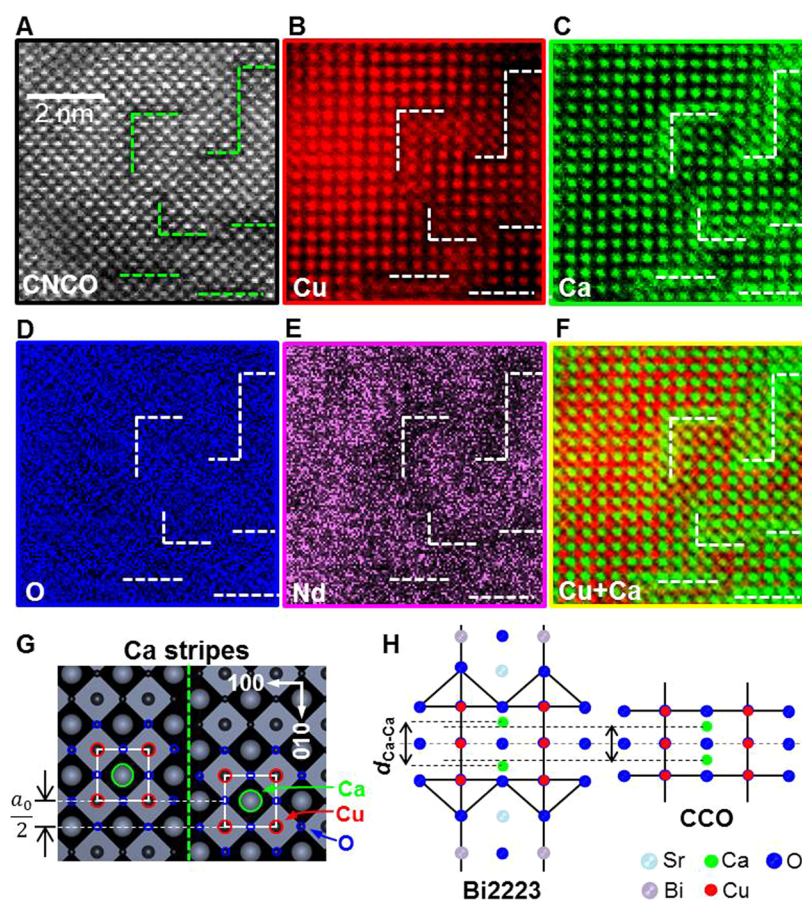
Figure 3. (A) High-resolution STEM and energy-dispersive spectrometry (EDS)-mapped CuO_2 planes found in $Ca_{0.96}Nd_{0.04}CuO_2$. (B–E) Elemental distributions of Cu, Ca, O, and Nd, respectively. (F) Combined elemental map of Cu and Ca. Dashed lines represent irregularities and demonstrate the distortions of the CuO_2 planes in $Ca_{0.96}Nd_{0.04}CuO_2$. This is schematically shown in (G), where the CuO_2 planes are distorted by the presence of Ca at the Cu site. In $Bi_2Sr_2Ca_2Cu_3O_{10+\delta}$, the position of Ca between the CuO_2 planes is slightly off its centric position[51,52] and the equilibrium position is different from what is observed in the infinite-layer $CaCuO_2$ phase.

conductivity while maintaining a static stripe structure is the "1/8-anomaly" in bulk $La_{2-x}Ba_xCuO_4$.[37–41] As IL-$CaCuO_2$ is a cuprate with square-planar coordinated copper, zone I is of higher importance. Notably, the apical positions of these cuprates are vacant and their absence gives rise that the copper ions are not susceptible to Jahn–Teller distortions per se (JT free). Commonly, these cuprates crystallize in the T′ structure with $d_{Cu-O} > d_B$. The large d_{Cu-O} keeps cuprates with T′ structure away from cationic stripe formation, while being still perceptible to electronic stripes.[42,43] Instead, the T′ structure is known to be prone to point defects, so-called interstitial oxygen atoms, preventing superconductivity, which may be also the case with IL cuprates. Oxygen vacancies, if any, also matter as exemplified by the work by Leca et al.,[44] who grew superconducting IL cuprate films in a low oxidizing atmosphere and oxidized them after the growth. Solutions are, nonetheless, in place to eliminate such defects and instigate superconductivity. In IL-$SrCuO_2$, d_{Cu-O} almost coincides with d_B, and cationic replacement of Sr by La places d_{Cu-O} comfortably above d_B and gives rise to super-conductivity. Note that any substitution of Ca in IL-$Ca_{1-x}R_xCuO_2$ (R = La, Nd, Sr) does not sufficiently expand d_{Cu-O} so that $d_{Cu-O} > d_B$.

In strict terms, four- and five-coordinated copper is not Jahn–Teller-active. Nonetheless, weak Jahn–Teller activities for four- and five-coordinated copper are known[11,45,46] and IL-

$Ca_{1-x}R_xCuO_2$ has a d_{Cu-O}, where such influences are common. One might be inclined to raise the question as to why such a structure does even exist. The synthesis conditions of IL cuprates[1,3,5] are significantly off from thermodynamic equilibrium conditions. Moreover, the square-planar configuration of Cu^{2+} is rare among copper complexes[47,48] and infinitely connected CuO_4 strata are only known for IL and T′ structure cuprates. The famous compound, Egyptian Blue (CaCu-Si_4O_{10}), does have square CuO_4 plaquettes with $d_{Cu-O} \approx$ 1.928 Å, (equal to IL-$CaCuO_2$) though they are not infinitely connected.[49,50] After all, the IL-$Ca_{1-x}R_xCuO_2$ system must be considered as metastable and highly susceptible to structural distortions driven by the Jahn–Teller effect to lower the energy of this crystallographic system. These effects cumulate in the formation of cationic stripes within the CuO_2 planes and this is irreconcilable with superconductivity.

Superconducting cuprates located in zone II, particularly those with very high T_c ($HgBa_2Ca_2Cu_3O_{8+\delta}$, $Tl_2Ba_2Ca_2Cu_3O_{10+\delta}$, and $Bi_2Sr_2Ca_2Cu_3O_{10+\delta}$), accommodate a modified IL-$CaCuO_2$, where the calcium ions are now shifted further away from the CuO_2 plane (Figure 3H), and this modification is sufficient to lower the local symmetry of the system. For example, in $Bi_2Sr_2Ca_2Cu_3O_{10+\delta}$, the infinite layer is sandwiched between $BiO_{1.5+\delta}$ layers that are sufficiently potent to outweigh local charge imbalances nascent from crystallographic imperfections, a function unachievable in the plain
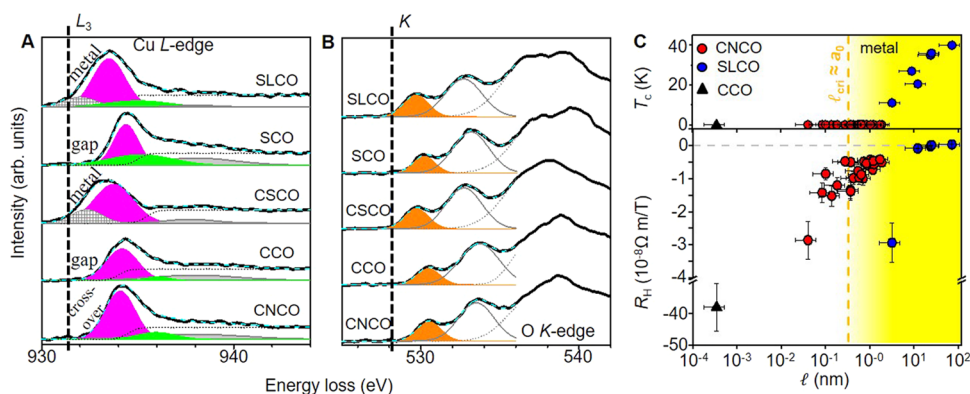
Figure 4. (A) Electron energy loss spectra of Cu and O embedded in CuO_2 planes with Cu in a square-planar coordination environment. Here, we used $CaCuO_2$, $SrCuO_2$ $Ca_{0.85}Sr_{0.15}CuO_2$, $Sr_{0.90}La_{0.10}CuO_2$, and $Ca_{0.96}Nd_{0.04}CuO_2$. The Cu L edge is affected by the effective polarization brought onto the CuO_2 plane by varying the effective electrostatic potential from Ca^{2+} through $Ca_{1-x}^{2+}Sr_x^{2+}$ ($x = 0.15$) to $Sr_{1-x}^{2+}La_x^{3+}$ ($x = 0.10$). For $Sr_{0.90}La_{0.10}CuO_2$, high-temperature superconductivity appears at $T_c = 41$ K. The insulating states of $CaCuO_2$ and $SrCuO_2$ are distinct. For IL-$CaCuO_2$ and IL-$Ca_{0.96}Nd_{0.04}CuO_2$, one-dimensional cationic stripes are present and interrupting the CuO_2 planes, whereas in $SrCuO_2$, such stripes are not observed. For $Ca_{0.85}Sr_{0.15}CuO_2$, the electronic response is at the brink of a metallic state. The electronic response function seen at the Cu L edge (A) corresponds exactly to the O K edge (B), where the distribution of spectral weight is identical. (C) Plot of the superconducting transition temperature T_c as a function of the mean-free path length l in $CaCuO_2$, $Sr_{0.90}La_{0.10}CuO_2$, and $Ca_{0.96}Nd_{0.04}CuO_2$. l is limited due to cationic stripes in the CuO_2 planes, and this relates to the appearance of superconductivity. For the induction of superconductivity, l is required to be at least 4 Å, which corresponds to the Cu–Cu distance (a_0) of the CuO_2 planes. For a small l, the Hall coefficient R_H is negative ($<-1\times10^{-8}$ Ωm/T), and for $R_H \approx 0$ Ωm/T, $l \approx 30$ nm. For $Bi_2Sr_2CaCu_2O_{8+\delta}$ and $Bi_2Sr_2Ca_2Cu_3O_{10+\delta}$, R_H is positive[59] with $l > 10$ nm.[60]

$CaCuO_2$ system. Actually, the distance between two adjacent CuO_2 planes that is coerced by adamant Ca^{2+} ions in IL-$CaCuO_2$ ($c = 3.1766$ Å) is, by far, shorter than what is seen in $Bi_2Sr_2Ca_2Cu_3O_{10+\delta}$ ($c = 3.3077$ Å).[53,54] Additionally, the bonds of $BiO_{1.5+\delta}$ are very adaptive,[54] in contrast to unmalleable calcium ions.

In cooperation, these two buffering mechanisms (the variable stoichiometry in $BiO_{1.5+\delta}$ and the tunability of the Ca equilibrium position) format the environment of copper in a way that tolerates the IL-$CaCuO_2$ strata to be stable in cuprates of zone II. In other words, for a given Jahn–Teller potential there exists a chemistry that maintains this crystal structure without violation of the CuO_2 plane stability and it is exactly this part that is missing for the infinite-layer phase of $CaCuO_2$.[55] In contrast to the general assumption where the Jahn–Teller effect is being considered as a consequence of the electronic degeneracy owed to an unconventional bonding scheme specific to cuprates to form infinitely connected CuO_2 planes,[56] it is the polarization of the chemicals above and below the CuO_2 planes that promote or quench the implicit Jahn–Teller instability. The fact that the electronic polarization counteracts Jahn–Teller distortions in cuprate superconductors which are, *de facto*, superlattices, results in structural rearrangements, i.e., stipes which is a commonly accepted mechanism in multiferroic systems.[57] Several local distortions are possible and one of them is suitable to stabilize an overall superstructure, i.e., stripe formation,[37] as observed here in IL-$Ca_{1-x}R_xCuO_2$. Those stripes take away the stabilizing criteria of the infinite-layer phase, thus resulting in a progressive self-distractive inroad of the CuO_2 planes. Regrettably, these aspects are not covered by methods commonly used to derive electronic response of materials, e.g., density functional theory.[58] However, Jahn–Teller effects are of sufficient strength to amplify related electronic properties by several orders of magnitude, as exemplified in $Dy(Fe,Mn)O_3$ perovskites.[35,58]

The remaining point to be clarified is how the presence or absence of cationic stripes is reflected in the electronic response functions of the IL cuprate system. We characterized T_c, the Hall coefficient R_H, and the mean-free path length l (see the Supporting Information) and combined those results with STEM electron energy loss spectroscopy data taken at the Cu L_3 and O K-edges (see the Supporting Information). For superconducting IL-$Sr_{0.90}La_{0.10}CuO_2$ there exist a finite density of states (DOS) at the Cu L_3 as well as the O K-edges (Figure 4A,B) and we assign a Cu $3d$–O $2p$ hybridized state at the Fermi level, as is a common procedure for transition-metal oxides.[61,62] Knowing that cationic stripes are blotching the CuO_2 planes of IL-$Ca_{0.96}Nd_{0.04}CuO_2$, this is expected to change. Indeed, the DOS at Cu L_3 as well as the O K-edges is strongly depleted. The consequence of such a low DOS should become apparent in the electronic transport behavior. For all IL-$Ca_{0.96}Nd_{0.04}CuO_2$ samples investigated here, l is at most 5 unit cells (Figure 4C) and this length is consistent with the cationic stripe density seen by in-plane STEM measurements (Figure 2). As expected, this situation becomes more dramatic for pristine IL-$CaCuO_2$. At the Fermi level, an electronic excitation gap appears while $l \ll 1$ u.c. Effectively, in IL-$CaCuO_2$, the polar environment around its CuO_2 planes prevents the formation of a metallic state, and so does IL-$SrCuO_2$. At the same time, the positive R_H seen for IL-$Sr_{0.90}La_{0.10}CuO_2$ turns negative. Interpolating between these extreme points by IL-$Ca_{0.85}Sr_{0.15}CuO_2$ shows a population of DOS at the Fermi level though electronic conduction is steadfastly insulating (Figure S1). This may also arise from a very minute difference in local oxygen sublattice perfection between IL-$Ca_{0.85}Sr_{0.15}CuO_2$ and two end members (IL-$CaCuO_2$ and IL-$SrCuO_2$), requiring more detailed investigations. If l is small, then R_H is negative and *vice versa*, and this correlation suggests that reconstruction of the CuO_2 planes, i.e., stripe formation, is the very reason for the absence of superconductivity in cuprate superconductors. It seems that this might not be different for IL-$SrCuO_2$. Its electron energy loss spectroscopy (EELS) spectra are almost identical to those of IL-$CaCuO_2$ or IL-$Ca_{0.96}Nd_{0.04}CuO_2$, whereas rabbets are not apparent from the in-plane STEM imagery. As d_{Cu-O} is

somewhat smaller than d_B, IL-SrCuO$_2$ appears to be at the brink of cationic stripe formation while the density of rabbets might be low enough to be considered as point defects. Hence, IL-SrCuO$_2$ is an antiferromagnetic insulator, both locally and globally (Figure S1).

CONCLUSIONS

We have proposed a concept that combines all cuprate superconductors into a singular phase diagram. The control parameters of this superconducting cuprate phase diagram are d_{Cu-O}, the polar character of the CuO$_2$ planes, and the Jahn–Teller instability. We argue that this concept has important predictions that are essential for the comprehension of cuprate superconductors, which are *de facto* superlattices.

First, the local crystal structure in the vicinity of the CuO$_2$ planes is determined by the Jahn–Teller instability and Pauling's second rule.[34] Notably, the CuO$_2$ planes are the playground of high-T_c superconductivity.

Second, doping aka substitution or addition of chemical elements modify the effective electronic polarization of the CRL and this change in polarization affects d_{Cu-O}. Heterovalent substitution, where additional electrons populate antibonding Cu 3d–O 2p orbitals, further modifies the effective polarization. The c-axis response of the cuprate is in no way influenced by substitution and simply follows Vegard's law.

Third, the Cu–O bond lengths of cuprates with CRLs appear in a way where the Jahn–Teller effect responded to the imposed polarization strength of the CRLs.

Forth, one could say that, within certain boundary conditions, there exists for every d_{Cu-O} a chemistry, which is sufficiently potent to balance the Jahn–Teller influences in a way that allows for infinitely connected CuO$_2$ planes, thus superconductivity.

Fifth, if this balance cannot be maintained, the entirety of the cuprate will surrender to the Jahn–Teller principle and form cationic stripes. In the case of IL-CaCuO$_2$ and IL-Ca$_{0.96}$Nd$_{0.04}$CuO$_2$ presented here, cationic stripes disrupt the CuO$_2$ planes and are consequently fatal to superconductivity.

Sixth, the commonly observed disorder of the CRL for cuprates with very high T_c is helpful[63] to effectively counteract charge imbalances stemming from point defects in the CuO$_2$ planes. These imperfections must be, however, limited to the CRL, not the CuO$_2$ planes.[64]

Finally, other order parameters, e.g., charge- and spin-density waves, the pseudogap, and long-range antiferromagnetic order (Table S1) are in no contradiction, though might be considered as a dressing of the superconducting state.

In this context, higher superconducting transition temperatures in cuprate material systems are reachable, and such an approach will require thin-film materials synthesis methods. To date, the common cuprate superconductor is a materials system, built by thermodynamic constraints that are defined by bulk synthesis methods. An elegant way to bypass those limits, while enabling novel cuprate material systems, are thin-film synthesis methods that cater to the need of a highly diversified stratification approach. A first step in this direction was done by Castro et al.,[65] using SrTiO$_3$ as a CRL. This new material, in its entirety inaccessible to bulk synthesis methods, is superconducting and more materials combinations should be considered to synthesize cuprates with higher T_c.

ASSOCIATED CONTENT

Supporting Information

The Supporting Information is available free of charge at https://pubs.acs.org/doi/10.1021/acsomega.1c01720.

> Growth of infinite-layer cuprates by molecular beam epitaxy; electronic transport measurements; superconducting Bi$_2$Sr$_2$CaCu$_2$O$_{8+\delta}$ crystals as well as related high-resolution in-plane scanning transmission electron microscope imagery; and energy scale calibration of electron energy loss spectroscopy at relevant oxygen energy levels (PDF)

AUTHOR INFORMATION

Corresponding Author

Yoshiharu Krockenberger − *NTT Basic Research Laboratories, NTT Corporation, Atsugi, Kanagawa 243-0198, Japan;* orcid.org/0000-0002-7801-2947; Email: yoshiharu.k@lab.ntt.co.jp

Authors

Ai Ikeda − *NTT Basic Research Laboratories, NTT Corporation, Atsugi, Kanagawa 243-0198, Japan*
Hideki Yamamoto − *NTT Basic Research Laboratories, NTT Corporation, Atsugi, Kanagawa 243-0198, Japan*

Complete contact information is available at:
https://pubs.acs.org/10.1021/acsomega.1c01720

Notes

The authors declare no competing financial interest.

ADDITIONAL NOTE

[a]There are contradicting reports on the superconducting state.[7,8]

REFERENCES

(1) Ikeda, A.; Krockenberger, Y.; Yamamoto, H. Molecular beam epitaxy of electron-doped infinite-layer Ca$_{1-x}$R$_x$CuO$_2$ thin films. *Phys. Rev. Mater.* **2019**, 3, No. 064803.

(2) Wang, Y.; Lany, S.; Ghanbaja, J.; Fagot-Revurat, Y.; Chen, Y. P.; Soldera, F.; Horwat, D.; Mücklich, F.; Pierson, J. F. Electronic structures of Cu$_2$O, Cu$_4$O$_3$, and CuO: A joint experimental and theoretical study. *Phys. Rev. B* **2016**, 94, No. 245418.

(3) Krockenberger, Y.; Sakuma, K.; Yamamoto, H. Molecular Beam Epitaxy and Transport Properties of Infinite-Layer Sr$_{0.90}$La$_{0.10}$CuO$_2$ Thin Films. *Appl. Phys. Express* **2012**, 5, No. 043101.

(4) Krockenberger, Y.; Yamamoto, H.; Tsukada, A.; Mitsuhashi, M.; Naito, M. Unconventional transport and superconducting properties in electron-doped cuprates. *Phys. Rev. B* **2012**, 85, No. 184502.

(5) Krockenberger, Y.; Ikeda, A.; Kumakura, K.; Yamamoto, H. Infinite-layer phase formation in the $Ca_{1-x}Sr_xCuO_2$ system by reactive molecular beam epitaxy. *J. Appl. Phys.* **2018**, *124*, No. 073905.

(6) She, J.-H.; Zaanen, J.; Bishop, A. R.; Balatsky, A. V. Stability of quantum critical points in the presence of competing orders. *Phys. Rev. B* **2010**, *82*, No. 165128.

(7) Araujo-Moreira, F.; Lisboa-Filho, P.; Zanetti, S.; Leite, E.; Ortiz, W. Superconductivity in sintered-polycrystalline $PrBa_2Cu_3$. *Phys. B* **2000**, *284-288*, 1033−1034.

(8) Zou, Z.; Oka, K.; Ito, T.; Nishihara, Y. Bulk Superconductivity in Single Crystals of $PrBa_2Cu_3O_x$. *Jpn. J. Appl. Phys.* **1997**, *36*, L18−L20.

(9) Mazin, I. I. Theoretical possibilities for superconductivity in $PrBa_2Cu_3O_7$. *Phys. Rev. B* **1999**, *60*, 92−95.

(10) Manthiram, A.; Zhu, Y. On the absence of superconductivity in $Gd_{2-x}Ce_xCuO_4$. *Phys. C* **1994**, *226*, 165−169.

(11) Bacci, M. Jahn-Teller effect in five-coordinated copper(II) complexes. *Chem. Phys.* **1986**, *104*, 191−199.

(12) Poccia, N.; Ricci, A.; Campi, G.; Fratini, M.; Puri, A.; Gioacchino, D. D.; Marcelli, A.; Reynolds, M.; Burghammer, M.; Saini, N. L.; Aeppli, G.; Bianconi, A. Optimum inhomogeneity of local lattice distortions in La_2CuO_{4+y}. *Proc. Natl. Acad. Sci. U.S.A.* **2012**, *109*, 15685−15690.

(13) Krockenberger, Y.; Eleazer, B.; Irie, H.; Yamamoto, H. Superconducting- and Insulating-Ground States in La_2CuO_4 Structural Isomers. *J. Phys. Soc. Jpn.* **2014**, *83*, No. 114602.

(14) Bianconi, A.; Bianconi, G.; Caprara, S.; Castro, D. D.; Oyanagi, H.; Saini, N. L. The stripe critical point for cuprates. *J. Phys.: Condens. Matter* **2000**, *12*, 10655−10666.

(15) Vishik, I. M.; et al. Phase competition in trisected super-conducting dome. *Proc. Natl. Acad. Sci. U.S.A.* **2012**, *109*, 18332−18337.

(16) Aranda, M. A. G. Crystal structures of Copper-Based High-T_c Superconductors. *Adv. Mater.* **1994**, *6*, 905−921.

(17) Müller-Buschbaum, H. The Crystal Chemistry of High-Temperature Oxide Superconductors and Materials with Related Structures. *Angew. Chem., Int. Ed.* **1989**, *28*, 1472−1493.

(18) Yvon, K.; François, M. Crystal structures of high-T_c oxides. *Z. Phys. B: Condens. Matter* **1989**, *76*, 413−444.

(19) Park, C.; Snyder, R. L. Structures of High-Temperature Cuprate Superconductors. *J. Am. Ceram. Soc.* **1995**, *78*, 3171−3194.

(20) Siemons, W.; Koster, G.; Blank, D. H. A.; Hammond, R. H.; Geballe, T. H.; Beasley, M. R. Tetragonal CuO: End member of the 3d transition metal monoxides. *Phys. Rev. B* **2009**, *79*, No. 195122.

(21) Moser, S.; Shaik, N. E.; Samal, D.; Fatale, S.; Dalla Piazza, B.; Dantz, M.; Pelliciari, J.; Olalde-Velasco, P.; Schmitt, T.; Koster, G.; Mila, F.; Rønnow, H. M.; Grioni, M. Magnons in tetragonal CuO. *Phys. Rev. B* **2015**, *92*, No. 140404.

(22) Samal, D.; Tan, H.; Takamura, Y.; Siemons, W.; Verbeeck, J.; Van Tendeloo, G.; Arenholz, E.; Jenkins, C. A.; Rijnders, G.; Koster, G. Direct structural and spectroscopic investigation of ultrathin films of tetragonal CuO: Six-fold coordinated copper. *EPL* **2014**, *105*, No. 17003.

(23) Jang, H.; Asano, S.; Fujita, M.; Hashimoto, M.; Lu, D. H.; Burns, C. A.; Kao, C.-C.; Lee, J.-S. Superconductivity-Insensitive Order at $q \sim 1/4$ in Electron-Doped Cuprates. *Phys. Rev. X* **2017**, *7*, No. 041066.

(24) Huang, E. W.; Mendl, C. B.; Liu, S.; Johnston, S.; Jiang, H.-C.; Moritz, B.; Devereaux, T. P. Numerical evidence of fluctuating stripes in the normal state of high-Tc cuprate superconductors. *Science* **2017**, *358*, 1161−1164.

(25) Martins, G. B.; Gazza, C.; Xavier, J. C.; Feiguin, A.; Dagotto, E. Doped Stripes in Models for the Cuprates Emerging from the One-Hole Properties of the Insulator. *Phys. Rev. Lett.* **2000**, *84*, 5844−5847.

(26) Wu, H.-H.; Buchholz, M.; Trabant, C.; Chang, C. F.; Komarek, A. C.; Heigl, F.; Zimmermann, M.; Cwik, M.; Nakamura, F.; Braden, M.; Schüßler-Langeheine, C. Charge stripe order near the surface of 12-percent doped $La_{2-x}Sr_xCuO_4$. *Nat. Commun.* **2012**, *3*, No. 1023.

(27) Berg, E.; Fradkin, E.; Kivelson, S. A.; Tranquada, J. M. Striped superconductors: how spin, charge and superconducting orders intertwine in the cuprates. *New J. Phys.* **2009**, *11*, No. 115004.

(28) Campi, G.; Bianconi, A.; Poccia, N.; Bianconi, G.; Barba, L.; Arrighetti, G.; Innocenti, D.; Karpinski, J.; Zhigadlo, N. D.; Kazakov, S. M.; Burghammer, M.; Zimmermann, M.; Sprung, M.; Ricci, A. Inhomogeneity of charge-density-wave order and quenched disorder in a high-T_c superconductor. *Nature* **2015**, *525*, 359−362.

(29) Giraldo-Gallo, P.; Zhang, Y.; Parra, C.; Manoharan, H. C.; Beasley, M. R.; Geballe, T. H.; Kramer, M. J.; Fisher, I. R. Stripe-like nanoscale structural phase separation in superconducting $BaPb_{1-x}Bi_xO_3$. *Nat. Commun.* **2015**, *6*, No. 8231.

(30) Wolf, D. Structure of ionic interfaces from an absolutely convergent solution of the Madelung problem. *Solid State Ionics* **1995**, *75*, 3−11.

(31) Suter, A.; Logvenov, G.; Boris, A. V.; Baiutti, F.; Wrobel, F.; Howald, L.; Stilp, E.; Salman, Z.; Prokscha, T.; Keimer, B. Superconductivity drives magnetism in δ-doped La_2CuO_4. *Phys. Rev. B* **2018**, *97*, No. 134522.

(32) Veyssière, P.; Rabier, J.; Grilhé, J. Stacking fault energy computations in oxides with normal and inverse spinel structures. *Phys. Status Solidi A* **1975**, *31*, 605−614.

(33) Kalinin, S. V.; Spaldin, N. A. Functional Ion Defects in Transition Metal Oxides. *Science* **2013**, *341*, 858−859.

(34) Pauling, L. THE PRINCIPLES DETERMINING THE STRUCTURE OF COMPLEX IONIC CRYSTALS. *J. Am. Chem. Soc.* **1929**, *51*, 1010−1026.

(35) Halcrow, M. A. Jahn−Teller distortions in transition metal compounds, and their importance in functional molecular and inorganic materials. *Chem. Soc. Rev.* **2013**, *42*, 1784−1795.

(36) *Phase Transitions and Self-Organization in Electronic and Molecular Networks*; Phillips, J. C.; Thorpe, M. F., Eds.; Fundamental Materials Research; Springer: US, 2001.

(37) Oyanagi, H.; Zhang, C. Local Lattice Distortion in Super-conducting Cuprates Studied by XAS. *J. Phys.: Conf. Ser.* **2013**, *428*, No. 012042.

(38) Chen, X. M.; Thampy, V.; Mazzoli, C.; Barbour, A. M.; Miao, H.; Gu, G. D.; Cao, Y.; Tranquada, J. M.; Dean, M. P. M.; Wilkins, S. B. Remarkable Stability of Charge Density Wave Order in $La_{1.875}Ba_{0.125}CuO_4$. *Phys. Rev. Lett.* **2016**, *117*, No. 167001.

(39) Bianconi, A.; Bianconi, G.; Caprara, S.; Castro, D. D.; Oyanagi, H.; Saini, N. L. The stripe critical point for cuprates. *J. Phys.: Condens. Matter* **2000**, *12*, 10655−10666.

(40) Suyolcu, Y. E.; Wang, Y.; Sigle, W.; Baiutti, F.; Cristiani, G.; Logvenov, G.; Maier, J.; Aken, P. A. Octahedral Distortions at High-Temperature Superconducting La_2CuO_4 Interfaces: Visualizing Jahn−Teller Effects. *Adv. Mater. Interfaces* **2017**, *4*, No. 1700737.

(41) Baiutti, F.; Logvenov, G.; Gregori, G.; Cristiani, G.; Wang, Y.; Sigle, W.; van Aken, P. A.; Maier, J. High-temperature super-conductivity in space-charge regions of lanthanum cuprate induced by two-dimensional doping. *Nat. Commun.* **2015**, *6*, No. 8586.

(42) Sadori, A.; Grilli, M. Stripe Formation in Electron-Doped Cuprates. *Phys. Rev. Lett.* **2000**, *84*, 5375−5378.

(43) Raczkowski, M.; Oleś, A. M.; Frésard, R. Stripe phases—possible ground state of the high-T_c superconductors. *Low Temp. Phys.* **2006**, *32*, 305−319.

(44) Leca, V.; Blank, D. H. A.; Rijnders, G.; Bals, S.; van Tendeloo, G. Superconducting single-phase $Sr_{1-x}La_xCuO_2$ thin films with improved crystallinity grown by pulsed laser deposition. *Appl. Phys. Lett.* **2006**, *89*, No. 092504.

(45) Sturge, M. The Jahn-Teller Effect in Solids. In *Solid State Physics*; Seitz, F.; Turnbull, D.; Ehrenreich, H., Eds.; Academic Press, 1968; Vol. *20*, pp 91−211.

(46) Hitchman, M. A. The Influence of Vibronic Coupling on the Spectroscopic Properties and Stereochemistry of Simple 4- and 6-Coordinate Copper(II) Complexes. *Comments Inorg. Chem.* **1994**, *15*, 197−254.

(47) Waroquiers, D.; Gonze, X.; Rignanese, G.-M.; Welker-Nieuwoudt, C.; Rosowski, F.; Göbel, M.; Schenk, S.; Degelmann,

P.; André, R.; Glaum, R.; Hautier, G. Statistical Analysis of Coordination Environments in Oxides. *Chem. Mater.* **2017**, *29*, 8346−8360.

(48) Gray, H. B.; Ballhausen, C. J. A Molecular Orbital Theory for Square Planar Metal Complexes. *J. Am. Chem. Soc.* **1963**, *85*, 260−265.

(49) García-Fernández, P.; Moreno, M.; Aramburu, J. A. Origin of the Exotic Blue Color of Copper-Containing Historical Pigments. *Inorg. Chem.* **2015**, *54*, 192−199.

(50) Sebastian, S. E.; Harrison, N.; Batista, C. D.; Balicas, L.; Jaime, M.; Sharma, P. A.; Kawashima, N.; Fisher, I. R. Dimensional reduction at a quantum critical point. *Nature* **2006**, *441*, 617−620.

(51) Watanabe, T.; Fujii, T.; Matsuda, A. Structural Study of Inhomogeneous Charge Distribution of Inequivalent CuO_2 Planes in $Bi_{2.1}Sr_{1.9}Ca_2Cu_3O_{10+\delta}$ Single Crystals. *J. Phys. Soc. Jpn.* **2003**, *72*, 2924−2929.

(52) HERVIEU, M.; MICHEL, C.; DOMENGES, B.; LALIGANT, Y.; LEBAIL, A.; FEREY, G.; RAVEAU, B. ELECTRON MICROSCOPY STUDY OF THE SUPERCONDUCTOR $Bi_2Sr_2CaCu_2O_{8+\delta}$. *Mod. Phys. Lett. B* **1988**, *02*, 491−500.

(53) Kovaleva, N. N.; Boris, A. V.; Holden, T.; Ulrich, C.; Liang, B.; Lin, C. T.; Keimer, B.; Bernhard, C.; Tallon, J. L.; Munzar, D.; Stoneham, A. M. *c*-axis lattice dynamics in Bi-based cuprate superconductors. *Phys. Rev. B* **2004**, *69*, No. 054511.

(54) Shamray, V. F.; Mikhailova, A. B.; Mitin, A. V. Crystal structure and superconductivity of Bi-2223. *Crystallogr. Rep.* **2009**, *54*, 584−590.

(55) Falvello, L. R. Jahn−Teller effects in solid-state co-ordination chemistry. *J. Chem. Soc., Dalton Trans.* **1997**, 4463−4476.

(56) Keller, H.; Bussmann-Holder, A.; Müller, K. A. Jahn−Teller physics and high-Tc superconductivity. *Mater. Today* **2008**, *11*, 38−46.

(57) Chen, L.; Xu, C.; Tian, H.; Xiang, H.; Íñiguez, J.; Yang, Y.; Bellaiche, L. Electric-Field Control of Magnetization, Jahn-Teller Distortion, and Orbital Ordering in Ferroelectric Ferromagnets. *Phys. Rev. Lett.* **2019**, *122*, No. 247701.

(58) Bersuker, I. B. The Jahn-Teller and pseudo Jahn-Teller effect in materials science. *J. Phys.: Conf. Ser.* **2017**, *833*, No. 012001.

(59) Khassanov, I.; Hopfengärtner, R.; Nakano, H.; Saemann-Ischenko, G. *High Tc Superconductor Thin Films*; CORRERA, L., Ed.; Elsevier: Oxford, 1992; pp 61−65.

(60) Hedin, L.; Lee, J. D. External losses in photoemission from strongly correlated quasi-two-dimensional solids. *Phys. Rev. B* **2001**, *64*, No. 115109.

(61) Yedra, L.; Xuriguera, E.; Estrader, M.; López-Ortega, A.; Baró, M. D.; Nogués, J.; Roldan, M.; Varela, M.; Estradé, S.; Peiró, F.; et al. Oxide Wizard: An EELS Application to Characterize the White Lines of Transition Metal Edges. *Microsc. Microanal.* **2014**, *20*, 698−705.

(62) Tao, R.; Todorovic, R.; Liu, J.; Meyer, R. J.; Arnold, A.; Walkosz, W.; Zapol, P.; Romanenko, A.; Cooley, L. D.; Klie, R. F. Electron energy-loss spectroscopy study of metallic Nb and Nb oxides. *J. Appl. Phys.* **2011**, *110*, No. 124313.

(63) Leroux, M.; Mishra, V.; Ruff, J. P. C.; Claus, H.; Smylie, M. P.; Opagiste, C.; Rodière, P.; Kayani, A.; Gu, G. D.; Tranquada, J. M.; Kwok, W.-K.; Islam, Z.; Welp, U. Disorder raises the critical temperature of a cuprate superconductor. *Proc. Natl. Acad. Sci. U.S.A.* **2019**, *116*, 10691−10697.

(64) Oku, T. High-resolution electron microscopy and electron diffraction of perovskite-type superconducting copper oxides. *Nanotechnol. Rev.* **2014**, *3*, 413−444.

(65) Di Castro, D.; et al. Occurrence of a high-temperature superconducting phase in $(CaCuO_2)_n/(SrTiO_3)_m$ superlattices. *Phys. Rev. B* **2012**, *86*, No. 134524.